Preprints of the 2012 20th Mediterranean Conference on Control & Automation (MED), Barcelona, Spain, July 3-6, 2012

Stator Winding Short Circuit Fault Detection Based on Set Membership Identification for Three Phase Induction Motors

Mohammed Obaid Mustafa, George Nikolakopoulos, Thomas Gustafsson

Abstract— **In this article a fault detection scheme for stator winding short circuit fault detection in the case of a three phase induction motor is being presented. The three phase motor is being modeled in the equivalent two phase motor ($q-d$) space, while the modeling of the faulty case is being also formulated. The motor is being identified by the utilization of Set Membership Identification (SMI) that has the merit of identifying both the parameters of the motor as also providing uncertainty safety bounds by calculating orthotopes which bounds the systems parameter vector. Based on the volume and the trend of these orthotopes, rules for identifying the existence of a fault are being presented. If the current values of the identified parameters do not lie inside the safety bounds in the healthy case, but lie in an area that is being defined by the model of the short circuit case, then a fault is being triggered. Detailed analysis of the proposed approach as also extended simulation results are being presented that prove the efficiency of the suggested scheme.**

NOMENCLATURE

$V_{sa},\ V_{sb},\ V_{sc}$: Stator's three phase voltages (V)
$V_{ra},\ V_{rb},\ V_{rc}$: Rotor's three phase voltages (V)
$i_{ra},\ i_{rb},\ i_{rc}$: Rotor's three phase currents (A)
$i_{sa},\ i_{sb},\ i_{sc}$: Stator's three phase currents (A)
$r_s,\ r_r$: Resistance of stator's and rotor's winding (Ohm)
$L_{ss},\ L_{rr}$: Stator's and rotor's self–inductances ($Henry$)
$L_s,\ L_r$: Stator's and rotor's self inductance ($Henry$)
L_m : Mutual inductance ($Henry$)
ω_r : Rotor's angular speed (rad/sec)
ω_m : Rotor's speed (mechanical) (rad/sec)
ω_s: Supply angular frequency (rad/sec)
P : No. of poles pairs
J : Moment of inertia ($Kg \cdot m^2$)
T_L : Load torque (Nm)
T_e : Electromagnetic torque (Nm)
q : Quadrature axis frame
d : Direct axis frame
s : Stator quantities
r : Stator quantities
$\psi_s,\ \psi_r$: Stator's and Rotor's fluxes ($Weber$)
θ : Angular position in the frame of motor (Deg)
θ_r : Angle between rotor's phase axis and stator's phase axis
β : Angle between rotor's phase axis and stator's phase axis

I. INTRODUCTION

Induction motors are critical components in many industrial processes, while at the same time these motors pose significant advantages when compared to the DC and synchronous motors in aspects, such as size, efficiency, cost, life span and maintainability [1]. Moreover induction motors, which represent one of the enabling technologies, in the modern commercial and industrial processes, are sometimes referred to as the "workhorses of modern industry" [2], while in the recent years, the detailed study of their dynamic behavior, has received a significant consideration [3].

The most common faults that could be appeared in the rotor and the stator of an induction motor are: a) short circuit stator winding, b) broken rotor bars [4], and c) bearing failures and dynamic or static air gab irregularities [5]. From all these types of faults, the stator winding short–circuit faults comprise around 40% of all the reported motor faults. It is necessary to detect this type of fault, as soon as possible, since it has the potential to develop into a catastrophic system failure with an eventual significant damage to the motor's core [6, 7].

In the relative scientific literature there have been proposed multiple fault detection techniques that based their operation on: a) spectral analysis of stator currents [8] and b) stator voltage and electromagnetic torque [9]. These methods base their operation on the detection of spectrum lines at certain frequencies using classical methods like Fouriers analysis [10] and are quite simple to be implemented, while these methods have been applied widely for fixed speed applications. In industrial applications under varying speed and with a direct power supply, these methods are not well adapted because electrical signals are not stationary. Recently, continuous time identification has been used to perform diagnosis procedure, the objective of these methods was the detection of faults occurring in induction machines, these techniques study the deviation of parameters to detect and localize faults [9, 10].

In parallel to these fault detection schemes, Set Membership Identification (SMI) [11, 12] has received a growing attention in the past years suggesting a quite important technique for system identification with bounds of uncertainty. In the SMI scheme a priori assumptions about the corrupting noise in the system are being taken under consideration in order to constrain the identified parameters to certain sets. The adaptation capabilities of the recursive implementation of the SMI–algorithms suggest their usage in robust identification schemes, while several versions of SMI–algorithms have recently appeared in the literature [13–16], including different methodologies for bounding the uncertainty and with the capability of being calculated recursively and online.

M. Obaid, G. Nikolakopoulos and T. Gustafsson are with the Department of Computer Science, Electrical and Space Engineering, Division of Systems and interaction, Luleå University of Technology, Luleå, Sweden
Corresponding Author's Email: geonik@ltu.se

978-1-4673-2529-5/12/$31.00 ©2012 IEEE

The main novelty of this article stems from the adaptation of the SMI approach to the problem of fault detection and more specifically to the problem of detection stator winding short circuit detection. To the author's best knowledge this is the first time that such an approach is being reported in the scientific literature. The extension of this scheme to other types of fault can support a general fault detection framework, where fault diagnosis could be also performed in parallel with the fault detection scheme. The simplified modeling (two phase models) for the healthy and the faulty cases, and the safety intervals for the online SMI for the parameters, are establishing a robust fault detection scheme that could be directly transferred to real–life implementations.

The rest of the article is being structured as it follows. In Section II the model derivation and simplification, for the healthy and the faulty cases are being derived. In Section III the SMI scheme is being presented coupled with the reasoning rules for detecting the occurrence of a fault. In Section IV multiple simulation results that prove the efficacy of the proposed methodology are being presented, while the conclusions are drawn in the last Section V.

II. Induction Motor Modeling

A. Healthy Case

In general an induction motor can be modeled as a three phase model or as an equivalent quadrature phase model [17], while the voltage balance equations for the case of a three phase induction motor can be formulated as [18, 19]:

$$\mathbf{V} = \mathbf{p}\ \psi + \mathbf{R}\ \mathbf{i} \tag{1}$$

where

$$\begin{aligned} \psi &= [\psi_{sa}\ \psi_{sb}\ \psi_{sc}\ \psi_{ra}\ \psi_{rb}\ \psi_{rc}]^T && (2)\\ \mathbf{V} &= [V_{sa}\ V_{sb}\ V_{sc}\ V_{ra}\ V_{rb}\ V_{rc}]^T && (3)\\ \mathbf{i} &= [i_{sa}\ i_{sb}\ i_{sc}\ i_{ra}\ i_{rb}\ i_{rc}]^T && (4)\\ \mathbf{R} &= diag\left[\ r_s\ r_s\ r_s\ r_r\ r_r\ r_r\ \right] && (5) \end{aligned}$$

and $r_{sa} = r_{sb} = r_{sc}$ and $r_{ra} = r_{rb} = r_{rc}$ in the balance case of motor, the operator p is equal to the first derivative d/dt

$$\begin{aligned} V_{sa} &= V_m sin(\omega_s t)\\ V_{sb} &= V_m sin(\omega_s t - 2\pi/3) && (6)\\ V_{sc} &= V_m sin(\omega_s t - 4\pi/3) \end{aligned}$$

and the relation between the phase linkages and the phase currents is provided by: [19]

$$\psi = \mathbf{L}\ \mathbf{i} \tag{7}$$

In this formulation the values of the inductance matrix $\mathbf{L}$ depend on the rotor's electrical angle and the type of the utilized model [7]. For simplifying the three phase model, the equivalent two phase model will be extracted that has been converted to the $q-d$ coordination frame, as it has been presented in Figure 1 [20].

In this figure the schematic diagram of the 3–phase induction motor with the $d-q$ axes superimposed is being presented, where the q–axis lags the d–axis by 90^o. A voltage

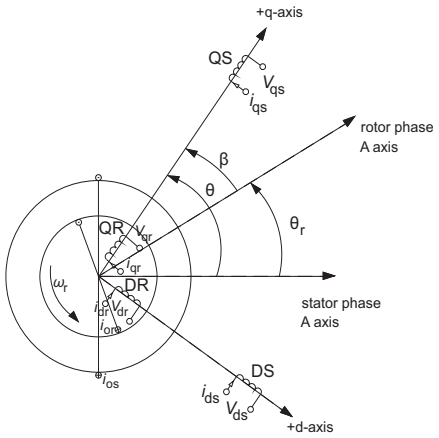

Fig. 1. q-d model of induction motor

V_{as} is applied to stator phase and the corresponding current flow is i_{as}. The phases b and c have not been presented on this scheme in an attempt to maintain clarity. In the $d-q$ model, the coils DS and QS replace the stator phase coils as, bs and cs, while coils DR and QR replace the rotor phase coils ar, br and cr. In Figure 1 only the four coils DS, QS, DR and QR are being presented to illustrate the simplification from the 3-phase induction motor with six coils to the case of a 2-phase induction motor with four coils. For predicting the mechanical and electrical behavior of the original machine correctly, the original abc variables F_{abc} must be transformed into the $d-q$ variables F_{qdo} and this is being carried out through Park's transform as it follows [21]:

$$\begin{aligned} \mathbf{F_{dqo}} &= \mathbf{T_{qdo}} \cdot \mathbf{F_{abc}} && (8)\\ \mathbf{V_{dqo}} &= \mathbf{T_{qdo}} \cdot \mathbf{V_{abc}} && (9)\\ \mathbf{i_{dqo}} &= \mathbf{T_{qdo}} \cdot \mathbf{i_{abc}} && (10) \end{aligned}$$

where

$$\mathbf{T_{dqo}} = \frac{\mathbf{2}}{\mathbf{3}} \begin{bmatrix} \cos\theta & \cos\theta_1 & \cos\theta_2 \\ \sin\theta & \sin\theta_1 & \sin\theta_2 \\ 1/2 & 1/2 & 1/2 \end{bmatrix} \tag{11}$$

and

$$\begin{aligned} \mathbf{V_{dqo}} &= [\mathbf{v_q}\ \ \mathbf{v_d}\ \ \mathbf{v_0}]^\mathbf{T} && (12)\\ \mathbf{i_{dqo}} &= [\mathbf{i_q}\ \ \mathbf{i_d}\ \ \mathbf{i_0}]^\mathbf{T} && (13) \end{aligned}$$

with $\theta_1 = \theta - 2\pi/3$, $\theta_2 = \theta - 4\pi/3$. In the case that the saturation and the fraction effects are being neglected, the balance voltage equation of the three phase induction motor in $q-d$ model are provided by:

$$\mathbf{L_{qd}}\ \mathbf{pi^{sr}_{qd}} = \mathbf{V^{sr}_{qd}} - \mathbf{R_{qd}} \mathbf{i^{sr}_{qd}} \tag{14}$$

and the $\mathbf{pi^{sr}_{qd}}$ can be calculated as:

$$\mathbf{pi^{sr}_{qd}} = -\mathbf{L^{-1}_{qd}} \mathbf{R_{qd}} \mathbf{i^{sr}_{qd}} + \mathbf{L^{-1}_{qd}} \mathbf{V^{sr}_{qd}} \tag{15}$$

where

$$\mathbf{V_{qd}^{sr}} = [v_{qs} \;\; v_{ds} \;\; v_{qr} \;\; v_{dr}]^T \quad (16)$$

$$\mathbf{i_{qd}^{sr}} = [i_{qs} \;\; i_{ds} \;\; i_{qr} \;\; i_{dr}]^T \quad (17)$$

$$\mathbf{L_{qd}} = \begin{bmatrix} L_s & 0 & L_m & 0 \\ 0 & L_s & 0 & L_m \\ L_m & 0 & L_r & 0 \\ 0 & L_m & 0 & L_r \end{bmatrix} \quad (18)$$

and

$$\mathbf{R_{qd}} = \begin{bmatrix} r_s & 0 & 0 & 0 \\ 0 & r_s & 0 & 0 \\ 0 & -\omega_r/\omega_s \; L_m & rr & -\omega_s/\omega_s \; L_r \\ \omega_r/\omega_s \; L_m & 0 & \omega_r/\omega_s \; L_r & rr \end{bmatrix} \quad (19)$$

After these formulations, equation (18) can be re–written in a state space form as:

$$\begin{bmatrix} \frac{di_{qs}}{dt} \\ \frac{di_{ds}}{dt} \\ \frac{di_{qr}}{dt} \\ \frac{di_{dr}}{dt} \end{bmatrix} = A \begin{bmatrix} i_{qs} \\ i_{ds} \\ i_{qr} \\ i_{dr} \end{bmatrix} + B \begin{bmatrix} V_{qs} \\ V_{qr} \\ 0 \\ 0 \end{bmatrix} \quad (20)$$

where:

$$\mathbf{A} = -\mathbf{R_{qd}}\mathbf{L_{qd}}^{-1} \quad (21)$$

$$\mathbf{B} = \mathbf{L_{qd}}^{-1} \quad (22)$$

and with the **A** and **B** matrices defined as:

$$\mathbf{A} = \frac{1}{\delta}\begin{bmatrix} -L_r \; r_s & 0 & L_m \; r_s & 0 \\ 0 & -L_r \; r_s & 0 & L_m \; r_s \\ L_m \; r_r & 0 & -L_s \; r_r & w_r \; \delta \\ 0 & L_m \; r_r & -w_r \; \delta & -L_s \; r_r \end{bmatrix} \quad (23)$$

$$\mathbf{B} = \frac{1}{\delta}\begin{bmatrix} L_r & 0 & -L_m & 0 \\ 0 & L_r & 0 & -L_m \\ -L_m & 0 & L_s & 0 \\ 0 & -L_m & 0 & L_s \end{bmatrix} \quad (24)$$

and δ defined as:

$$\delta = L_s \; L_r - Lm^2 \quad (25)$$

Finally, the resulting equations for the torque and the motor's accelerations for the three phase induction motor are:

$$T_e = \frac{3}{2} \; P \; L_m[i_{qs} \; i_{dr} - i_{qr} \; i_{ds}] \quad (26)$$

In the presented formulation the fraction effect has been neglected and the equation of the mechanical angular speed will become:

$$J \; \frac{d\omega_m}{dt} = \; T_e - T_L \quad (27)$$

B. Stator Winding Short Circuit Modeling

Although induction motors are reliable electric machines, they are susceptible to many electrical and mechanical types of faults [5]. Electrical faults include stator faults resulting in the opening or shorting of one or more of a stator phase winding, broken rotor bars, and broken end rings, while mechanical faults include bearing failures and rotor eccentricities[1]. The focus of this research effort is on the stator faults during short circuit between stator winding, which happen in one phase of the motor. In the examined case all the stator parameters are considered to be identical when short circuit happens in the winding of the three phase induction motor, while both stator's resistance and inductance, as also the mutual inductances between stator and rotor will be directly affected.

In the case of such a fault, the modified (faulty) versions of matrices $\mathbf{A}^*$ and $\mathbf{B}^*$ should be utilized. In this case the $q-d$ reference frame transformation needs to be performed to these equations and by assuming that the short circuit occurs only in phase a of the stator for simplicity reasons and without loosing generality, the resistance matrix of stator with shorted turns in the $q-d$ reference frame can be derived as [7]:

$$\mathbf{r_{sf}^{qd0}} = \; r_s \begin{bmatrix} r_{s11} & 0 & r_{s13} \\ 0 & r_{s22} & 0 \\ r_{s31} & 0 & r_{s33} \end{bmatrix} \quad (28)$$

where $\mathbf{r_{sf}^{qd0}}$ is the stator winding resistance matrix in the faulty case. Let g_{sa} be the percentage of the remaining un–shorted stator windings in stator phase a and the non–zero elements of the matrix $\mathbf{r_{sf}^{qd0}}$ are being defined as [7]:

$$r_{s11} = \frac{1}{3}(2g_{as}+1) \;\; , \;\; r_{s13} = \frac{2}{3}(g_{as}-1) \; , \; r_{s22} = 1$$

$$r_{s31} = \frac{1}{3}(g_{as}-1) \; , \; r_{s33} = \frac{1}{3}(g_{as}+1) \quad (29)$$

while the inductance matrix in the faulty case will become as [7]:

$$\mathbf{L_f^*} = \begin{bmatrix} L_{11} & 0 & L_{14} & 0 \\ 0 & L_{22} & 0 & L_{25} \\ L_{41} & 0 & L_{44} & 0 \\ 0 & L_{52} & 0 & L_{55} \end{bmatrix} \quad (30)$$

where the elements of $\mathbf{L_f^*}$ are being defined as [7]:

$$L_{11} = \frac{1}{3}(g_{as}+1)L_s + \frac{1}{9}(2g_{as}+1)^2 \; L_s \quad (31)$$

$$L_{14} = L_{41} = \frac{1}{3}(g_{as}+1)L_m \; , \; L_{22} = L_s + L_m \quad (32)$$

$$L_{25} = L_{52} = L_m \; , \; L_{44} = L_{55} = L_r + L_m \quad (33)$$

and

$$\mathbf{R_f}^* = \begin{bmatrix} r^* & 0 & 0 & 0 \\ 0 & r_s & 0 & 0 \\ 0 & -\omega_r/\omega_s \; L_m^* & rr & -\omega_s/\omega_s \; L_r \\ \omega_r/\omega_s \; L_m^* & 0 & \omega_r/\omega_s \; L_r & rr \end{bmatrix} \quad (34)$$

with:

$$r^* = r_s \cdot r_{s11} \quad (35)$$

$$L_m^* = L_m \cdot L_{14} \quad (36)$$

Therefore the matrices $\mathbf{A}^*$ and $\mathbf{B}^*$ in the faulty case will change and become:

$$\mathbf{A}^* = -\mathbf{R_f^*} \; \mathbf{L_f^{*-1}} \quad (37)$$

$$\mathbf{B}^* = \mathbf{L_f^{*-1}} \quad (38)$$

For applying the suggested fault detection scheme the 2–phase model of the induction motor is being transformed to

a MIMO ARMA system:

$$\begin{bmatrix} \dot{i}_{qs}(t) \\ \dot{i}_{ds}(t) \\ \dot{i}_{qr}(t) \\ \dot{i}_{dr}(t) \end{bmatrix} = \begin{bmatrix} \theta_{qs}(t) \\ \theta_{ds}(t) \\ \theta_{qr}(t) \\ \theta_{dr}(t) \end{bmatrix}^T \cdot \begin{bmatrix} \Phi_{qs}(t) \\ \Phi_{ds}(t) \\ \Phi_{qr}(t) \\ \Phi_{dr}(t) \end{bmatrix}^T + \begin{bmatrix} e_{qs}(t) \\ e_{ds}(t) \\ e_{qr}(t) \\ e_{dr}(t) \end{bmatrix}^T \quad (39)$$

where the parameter vector $\theta_j(t)$, with j taking values from $[qs,\ ds,\ qr,\ dr]$ is being defined as:

$$\theta_j^T(t) = [F_{j,1}(t)\ \ldots\ F_{n,1}(t),\ T_{j,1}(t),\ \ldots, T_{m,1}(t)]^T \quad (40)$$

with $n,\ m$ the order of the denominator's and numerator's polynomials respectively. The regression vector $\Phi_j(t)$ is formulated as:

$$\begin{aligned} \Phi_j^T(t) = (&-y_j(t-1)..... - y_j(t-n), \ldots, \\ &u_j(t+m-n-1),\ \ldots,\ u_j(t-n)) \end{aligned} \quad (41)$$

In equation (39) the disturbances corrupting the measurements have been also taken under consideration, with the assumption that the model dynamics are being affected by an additive error, being bounded by a priori bounds defined as:

$$\gamma_j ||e_j(t)||^2 \leq\ 1, \forall\ t \quad (42)$$

Finally, in this MIMO ARMA modeling approach, the parameters in equation (40) for the case of $j = qs$ in healthy case are being defined as it follows:

$$\begin{aligned} T_{qs,1} &= \frac{L_r}{\delta} \\ T_{qs,2} &= b_1(a_1 + 2a_4 + a_2 b_2) \\ T_{qs,3} &= b_1(a_4^2 - 2a_1 a_4 - a_5^2 + a_2 a_3 - a_2 b_2(a_1 + a_4)) \\ T_{qs,4} &= -b_1(a_1 a_4^2 - a_2 * a_3 * a_4 + a_1 * a_5^2 + \\ &\quad a_2 b_2(a_1 a_4 - a_2 a_3)] \\ F_{qs,1} &= -(2a_1 + 2a_4) \\ F_{qs,2} &= a_1^2 + 4a_1 a_4 - 2a_2 a_3 + a_4^2 + a_5^2 \\ F_{qs,3} &= -2a_1^2 a_4 + 2a_1 a_2 a_3 - 2a_1 a_4^2 \\ &\quad -2a_1 a_5^2 + 2a_2 a_3 a_4 \\ F_{qs,4} &= a_1^2 a_4^2 + a_1^2 a_5^2 - 2a_1 a_2 a_3 a_4 + a_2^2 a_3^2 \end{aligned}$$

with:

$$\begin{aligned} a_1 &= -(L_r\ r_s)/\delta\ ,\ a_2 = (L_m\ r_s)/\delta \\ a_3 &= (L_m\ r_r)/\delta \\ a_4 &= -(L_r\ r_r)/\delta \\ a_5 &= \omega_r \\ b_1 &= L_r/\delta \\ b_2 &= -L_m/\delta \end{aligned}$$

while by following the same formulation, the rest of the dependencies between the F_j and T_j and the ARMA formulation could be extracted.

III. Set Membership Fault Identification

Set membership identification (SMI) refers to a class of techniques for estimating parameters of linear systems or signal models under a priori information that constrains the solutions to certain sets. The objective of the SMI techniques is the determination of the feasible parameter set that contains the nominal parameter vector and is consistent with a linearly parameterizable model, the measurement data and the a priori known bounded noise–error. Due to the complexity in computing the feasible parameter set, the majority of the SMI methods aims at the determination of a more conveniently computable parametric set that outer bounds the feasible parameter set [11, 22].

The SMI technique is based on the Weighted Recursive Least Squares (WRLS) with a forgetting factor for identifying the $\hat{\theta}$ motor's parameters and can be formulated by the following double recursions [23] in the sample instance t and the MIMO case j as:

$$\begin{aligned} \hat{\theta}_j(t) &= \hat{\theta}_j(t-1) + K_j(t)(y_j(t) - \Phi_j^T(t)\theta_j(t-1)) \\ K_j(t) &= P_j(t)\Phi_j(t) = P_j(t-1)\Phi_j(t)(\lambda + \Phi_j^T(t)P_j(t-1)\phi_j(t))^{-1} \\ P_j(t) &= (I - K_j(t)\ \Phi_j^T(t))P_j(t-1)/\lambda \\ e_j(t) &= y_j(t) - \Phi_j^T(t)\theta_j(t-1) \\ G_j(t) &= \Phi_j^T(t)P_j(t-1)\Phi(t) \end{aligned}$$

where P_j is the covariance matrix. In the SMI approach the initial bounds γ for the corrupting noise $\varepsilon_j(t)$ are being re–calculated in every iteration. This optimization in the uncertainty description is evolving with the time, as the better the knowledge of the parameters is, the smaller these bounds are. For finding the optimal value of $\lambda_j^*(t)$ and fine tune the SMI algorithm and achieve convergence, the maximum positive root of the following equation should be calculated in each iteration:

$$\begin{aligned} F_j(\lambda_j) &= \alpha_{2,j}\lambda_j^2 + \alpha_{1,j}\lambda_j + \alpha_{0,j} \\ \alpha_{2,j} &= (\ell + n - 1)G_j^2 \\ \alpha_{1,j} &= (2\ell + 2n - 1 + \gamma_j\ e_j^2) - \xi_j\ \gamma_j\ G_j)G_j \\ \alpha_{0,j} &= (\ell + n) * (1 - \gamma_j\ e_j^2) - \xi_j\ G_j\ \gamma_j \\ \xi_j(t) &= \xi_j(t-1) + \frac{\lambda_j}{\gamma_j} - \frac{\lambda_j\ e_j}{1 - \lambda_j\ G_j} \end{aligned}$$

with $\ell = m + 1$. For finding the upper and lower boundary for the identified parameters, the uncertainty bound $\sigma_j(t)$, should be computed in every iteration. For delivering these bounds, the smallest orthotope that bounds the ellipsoidal uncertainty of the parameter and it is oriented parallel to the parameter coordinate axes and centered on the centroid of the ellipsoid is being calculated as:

$$\sigma_j(t) = \sqrt{diag(P_j(t))} \quad (43)$$

while the corresponding ellipsoid and the equation of the orthotope can be calculated from [11, 24]:

$$\Omega_j(t) = \{\theta_j\ :\ (\frac{1}{|\sigma_{j,k}(t)|})(\theta_{j,\ k} - \hat{\theta}_{j,\ k}(t)) \leq\ 1,\ k = 1, ..., n+m\}$$

Assuming the binary representation index o, with $o \in 0,\ \ldots,\ 2^{n+m}$,

$$o = \alpha_{n+m+1}2^{n+m+1} - 1 + \ldots + \alpha_2 2^1 + \alpha_1 2^0, \quad (44)$$

the orthotope's vertices $V_{j,\ o}^{n+m+1}(k)$, $o = 0, \ldots, 2^{n+m+1} - 1$ are related to the σ_j parameters as:

$$V_{j,\ o}^{p}(k) = \theta_j(t) + [\alpha_{j,\ n+m+1}^{*}\sigma_{j,\ n+m+1}(t), \ldots, \alpha_{j,\ 1}\sigma_{j,\ 1}(t)]^T$$

where $\alpha^*_{j,(\cdot)} = \begin{cases} + & \text{when } a_{j,\,(\cdot)} = 1 \\ - & \text{when } a_{j,\,(\cdot)} = 0 \end{cases}$, and the volume ratio of the ellipsoid is being calculated by:

$$B_j(t) = det^{-1}\ \frac{C_j(t)}{\xi_j(t)} \tag{45}$$

where $C_j(t) = P_j(t)^{-1}$.

During the established fault detection scheme, the parameters of the induction motor are being constantly tracked, while the corresponding confidence interval bounds are being updated. In the case of a stator short winding fault, the values of the identified parameters will be characterized by a jump and a constant drift from the converged nominal values of the motor, as also the new parameters's bounds (faulty case) will exceed the previous calculated bounds (healthy case), which is a direct indication of a fault occurrence. Based on the proposed SMI scheme for fault detection, the following rules are being established. It is assumed that the SMI scheme is providing smooth value updates for the identified parameters. If a time window t_1 is being defined, then after the convergence of the parameters, small changes in the identified values should be allowed. For the ad–hoc defined bound B_1 the following rule is being formulated:

$$\theta^o_j(t) - \overline{\hat{\theta}_j(t-t_1:t)}| \geq B_2 \tag{46}$$

Where $\theta^o_j(k)$ denotes the j–converged identified parameter ,the notation $\bar{\cdot}$ denotes a moving average time window of length T_{p1}. Another two rules can be defined, that are related with the volumes of the bounding ellipsoids and orthotopes. The aim is to track the corresponding volumes of the bounding ellipsoid/orthotope and allow only small changes, as in the opposite case, this should generate an event of a fault. By defining two ad–hoc boundaries as B_2 and B_3 the following rules can be formulated:

$$\Omega^{e,o}_j(k) - \overline{\Omega^e_j(t-t_2):t}| \geq B_2 \tag{47}$$

$$V^o_{ort}(t) - \overline{V_{ort}(t-t_3)} \geq B_3 \tag{48}$$

where $\Omega^{e,o}, V^o_{ort}$ are the converged value of the ellipsoid in healthy case.

IV. Simulation Results

For evaluating the performance of the proposed SMI scheme for fault detection, a model of an induction machine has been considered with characteristics depicted in Table 1.

TABLE I
INDUCTION MOTOR PARAMETERS

Pole Numbers	4	r_s	0.0616 per unit
Input Voltage	240V	r_r	0.0753 per unit
Frequency	50Hz	J	0.00155 Kg.m
L_r	0.019 per unit	L_s	0.019 per unit
L_m	0.01833 per unit		

The first simulation results, will focus in presenting the difference between the motor's health and faulty case where 20% of short circuit in stator winding in phase 'a' has been considered. Those differences in terms of stator currents, rotor angular speeds and torques are being presented in Figures 2, 3, and 4 respectively. In Figure 2 the difference

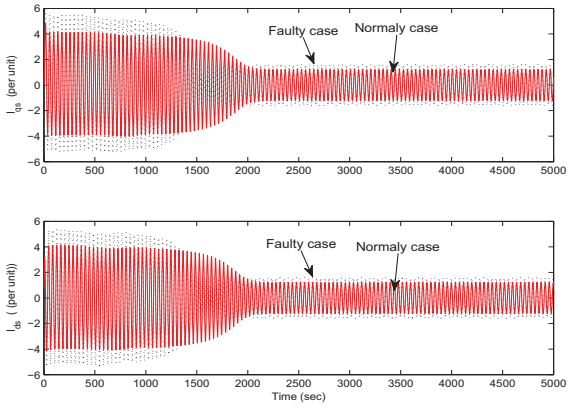

Fig. 2. The stator's and rotor's currents in the healthy and faulty case

between the healthy and the faulty cause is being presented, where it is obvious that the currents, both in the stator and in the rotor are being significantly increased in the case of a fault in the stator windings. In Figures 3 and 4 it is depicted that the fault is also affecting the steady values of the rotor's speed, which results also in a corresponding increase of the motor's temperature that might lead in additional faults, as also the steady state torque, where as it was depicted in the lower part of Figure 4, more oscillations are being appeared.

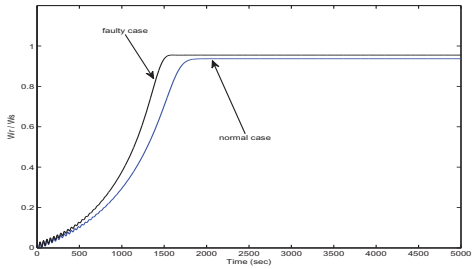

Fig. 3. The rotor angular speed of the motor in the healthy and faulty case

In the sequel, results from applying the proposed SMI scheme for fault detection are going to be presented. In Figures 5 and 6, the results from applying the SMI scheme on the healthy motor are being depicted, only for the case of having as input V_{qs} and output i_{qs}, while similar results have been obtained for the rest of the motor's parameters. As it can be observed from these figures the uncertainty bounds are starting from a large value and in the sequence, as the identification procedure is evolving and the identified parameters are close to the nominal values, those bounds are being decreased, until they reach their steady state value. It should be noted that due to the size of the bounds the exact

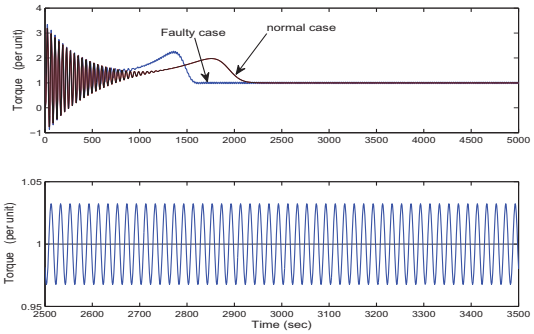

Fig. 4. The torque of the motor in the healthy and faulty case

values of the converged parameters is not clearly displayed in this Figure.

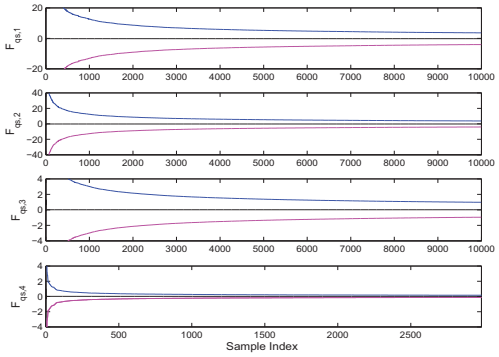

Fig. 5. SMI based identified parameters for F_{iqs} and corresponding uncertainty bounds

In Figure 7, the case of a fault occurred at 4800 samples (Sampling time $T_s = 0.01$) is being presented. Due to this fault, a jump in the identified parameters is taking place. Also it should be noted that in this case, the uncertainty intervals are changing (due to the drift in the identified model) and this leads in a bounds violation event, which indicates the existence of the fault. Similar graphs can also be extracted for all the identified parameters of the motor and without loosing generality, in Figure 7, only the results for $T_{ds,1}$ are being displayed.

The effectiveness of the identification scheme can also be examined by inspecting the volume of the bounding ellipsoid. As it is being displayed in Figure 8 the volume is being minimized and it is taking very small values as the identified model matches the real one. In the event of a fault, the identified values are being drifted to small values (resulting from the faulty model representation) and thus is why the bounds are being kept on monotonically being decreased. In general in a case of an extreme fault, these bounds would be significantly bigger and the event of the fault could be produced straight forward by simple monitoring the volume of the ellipsoids. In the case of the fault being produced by stator's short winding, the operation of the motor is still

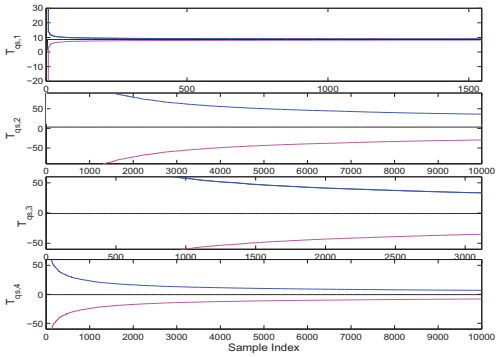

Fig. 6. SMI based identified parameters for T_{iqs} and corresponding uncertainty bounds

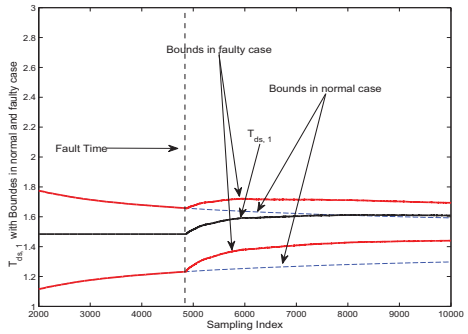

Fig. 7. Convergence of the $T_{ds,1}$ parameter and corresponding bounds before and after the occurrence of the fault

unaffected, and the result due to the fault is a parametric drift and thus the simple inspection of the volume should not be the only factor that should be monitored for fault identification. In this case, the occurrence of the fault has caused a jump on the ellipsoid volume, which was bigger than the a priori defined bound (100) and thus the algorithm is able to trigger a fault event.

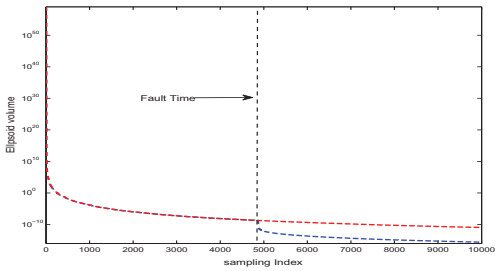

Fig. 8. Convergence of ellipsoid's volume and corresponding effect of the occurred fault

Finally, the effectiveness of the SMI scheme could also be examined by measuring the volume of the bounding orthotope. In Figure 9, the volumes of the polytopes generated for the $F_{qs,1}$ and $F_{qs,2}$ parameters are being displayed

in accordance with the sample index. As in the previous case, again the fault has generated an abnormal jump in the orthotopes volume. By simple tracking the distance among the centers of the polytopes and by applying the third rule in fault identification, again the event of the fault could also be triggered.

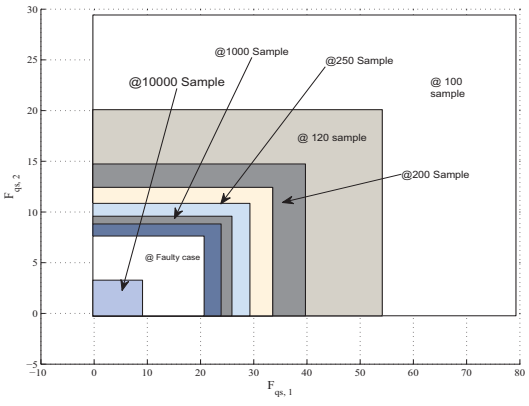

Fig. 9. Convergence of polytope's volume and corresponding effect of the occurred fault

V. Conclusions

In this article a fault detection scheme for stator winding short circuit fault detection in the case of a three phase induction motor has been presented. The three phase motor has been modeled in the equivalent two phase motor $(q-d)$ space, while the modeling of the faulty case has been also formulated. The motor has been identified by the utilization of the SMI algorithm that has the merit of identifying both the parameters of the motor as also providing uncertainty safety bounds by calculating orthotopes which bounds the systems parameter vector. Based on the volume and the trend of these orthotopes, rules for identifying the existence of a fault have been presented as also extended simulation results that proved the efficiency of the suggested scheme.

References

[1] B. Liang, B. Payne, A. Ball, and S. Iwnicki, "Simulation and fault detection of three-phase induction motors," *Mathematics and Computers in Simulation*, pp. 1–15, 2002.

[2] C. Laughman, B. Leeb, K. Norford, R. Shaw, and R. Armstrong, "A two step method for estimating the parameters of induction machine models," *IEEE Energy Conversion Congress and Exposition, ECCE 2009, San Jose, California*, no. art. no. 5316204, pp. 262–269, September 2009.

[3] M. Boucherma, M. Kaikaa, and A. Khezzar, "Park model of squirrel cage induction machine including space harmonics effects," *Journal of Electrical Engineering*, vol. 57 2006, 193199, no. 4, pp. 193–199, 2009.

[4] P. Santos and T. Lubiny, "A simplified induction machine model to study rotor broken bar effects and for detection," *European Transactions On Electrical Power*, vol. 20, p. 611, 2010.

[5] S. Nandi and H. Toliyat, "Condition monitoring and fault diagnosis of electrical machines-a review," *IEEE Transactions on Energy Conversion*, vol. 20, no. 4, pp. 719–729, Dec. 2005.

[6] J. Zafa and J. Gyselinck, "Cusum based fault detection of stator winding short circuits in doubly-fed induction generator based wind energy conversion systems," *International Conference on Renewable Energies and Power Quality (ICREPQ10) Granada (Spain)*, march.

[7] S. Chen and R. Zivanovic, "Modelling and simulation of stator and rotor fault conditions in induction machines for testing fault diagnostic techniques," *European Transactions On Electrical Power*, vol. 20, pp. 611 –629, April 2009.

[8] H. Douglas, P. Pillay, and A. Ziarani, "Detection of broken rotor bars in induction motors using wavelet analysis," *Electric Machines and Drives Conference, 2003. IEMDC'03. IEEE International*, pp. 923–928, July 2003.

[9] S. Bachi, S. Tnani, J. Trigeassou, and G. Champenois, "Diagnosis by parameter estimation of stator and rotor faults occurring in induction machines," *IEEE Transactions on Industrial Electronics*, vol. 53, no. 3, pp. 963–973, June 2006.

[10] S. Bachi, S. Tnani, T. Poinot, and J. Trigeassou, "Stator fault diagnosis in induction machines by parameter estimation," *Proc. IEEE Int.SDEMPED, Grado, Italy*, p. 235239, Sep. 2001.

[11] J. R. Deller, "Set membership identification in digital signal processing," *IEEE ASSP MAGAZINE*, vol. 6, no. 4, pp. 4–20, OCTOBER 1989.

[12] J. Deller, M. Nayeri, and S. Odeh, "Least–Square Identification with Error Bounds for Real–Time Signal Processing and Control," *Proceedings of the IEEE*, vol. 81, no. 6, pp. 815–849, Jun. 1993.

[13] M.-F. Cheung, S. Yurkovich, and K. Passino, "An optimal volume ellipsoid algorithm for parameter set estimation," *IEEE Transactions on Automatic Control*, vol. AC–38, no. 8, pp. 1292–1296, Aug. 1993.

[14] G. Belforte, B. Bona, and V. Cerone, "Parameter estimation algorithms for a set-membership description of uncertainty," *Automatica*, vol. 26, no. 5, pp. 887–898, 1990.

[15] A. Vicino and G. Zappa, "Sequential approximation of feasible parameter sets for identification with set membership uncertainty," *IEEE Transactions on Automatic Control*, vol. 41, pp. 774–783, Sep. 1996.

[16] J. Watkins and S. Yurkovich, "Parameter set estimation algorithms for time–varying systems," *International Journal of Control*, no. 5, pp. 711–732, Mar. 1997.

[17] M. Obaid, G. Nikolakopoulos, and T. Guastafsson, "A survey on modeling approaches for three phase induction motors," *The IASTED International Conference on Modelling, Simulation, and Identification , MSI 2011* , November 2011.

[18] P. VAS, *Electrical Machines and Drives*, O. S. PUBLICATION, Ed., 1992.

[19] A. Sarkar and G. Berg, "Digital simulation of three-phase induction motors," *IEEE Transactions on Power Apparatus and Systems*, vol. 89, no. 6, pp. 1031–1037, July/August 1970.

[20] K. Sandhu and V. Pahwa, "Sumilation study of three phase induction motor with variation in moment of inertia," *ARPN Journal of Enginering and Apllied Sciences*, vol. 4, no. 5, pp. 72–77, August 2009.

[21] R. Lee, P. Pillay, and R. Harley, "Dq reference frames for the simulation of induction motors," *Electric Power Systems Research*, vol. 8, pp. 15 –26, 1985.

[22] L. Ljung, *System Identification Theory For The User*. Englewood Cliffs, NJ: Prentice–Hall, 1987.

[23] F. Guastafsson, *Adaptive Filtering and Change Detection*, J. Wiley and Son, Eds., Sep.2001.

[24] K. Le, Z. Huang, C. Moon, and A. Tzes, "Fault detection based on orthotopic set membership identification for robot manipulators," *Proceedings of the 17th World Congress The International Federation of Automatic Control , Seoul, Korea,2008*, pp. 7344–7349, July 2008.